

# Infrared Photodissociation Spectra of Mass-Selected Homoleptic Dinuclear Palladium Carbonyl Cluster Cations in the Gas Phase<sup>†</sup>

Cui, Jieming<sup>a</sup>(崔洁铭) Xing, Xiaopeng<sup>b</sup>(邢小鹏) Chi, Chaoxian<sup>a</sup>(池超贤)  
 Wang, Guanjun<sup>a</sup>(王冠军) Liu, Zhipan<sup>\*a</sup>(刘智攀) Zhou, Mingfei<sup>\*a</sup>(周鸣飞)

<sup>a</sup> Department of Chemistry, Shanghai Key Laboratory of Molecular Catalysts and Innovative Materials, Fudan University, Shanghai 200433, China

<sup>b</sup> Graduate University of Chinese Academy of Sciences, College of Materials Sciences and Opto-Electronic Technology, Beijing 100049, China

Infrared spectra of mass-selected homoleptic dinuclear palladium carbonyl cluster cations  $\text{Pd}_2(\text{CO})_n^+$  ( $n=5-8$ ) are measured via infrared photodissociation spectroscopy in the carbonyl stretching frequency region. The structures are established by comparison of the experimental spectra with simulated spectra derived from density functional calculations. The  $\text{Pd}_2(\text{CO})_5^+$  cation is characterized to have two weakly semibridging CO groups with  $C_2$  symmetry. The  $\text{Pd}_2(\text{CO})_6^+$  and  $\text{Pd}_2(\text{CO})_7^+$  cations are determined to involve one weakly semibridging CO group. The  $\text{Pd}_2(\text{CO})_8^+$  cation is a CO coordination saturated cluster, which is determined to have a  $D_{2d}$  structure with all of the carbonyl groups terminally bonded. Bonding analysis indicates that these cluster cations each has a Pd—Pd half bond. The Pd—Pd distance increases with the number of CO ligands.

**Keywords** metal carbonyl cluster, palladium-palladium bonding, density functional calculation, infrared spectrum

## Introduction

Palladium is widely used as catalyst for carbon monoxide reduction and activation in many industrial processes. Thus, the interactions of charged and neutral palladium metal atoms, clusters, and surfaces with carbon monoxide and the resulting carbonyl complexes have received considerable experimental and theoretical attention. Mononuclear palladium carbonyl neutrals as well as ions have been produced in rare-gas matrices and studied with infrared absorption spectroscopy.<sup>[1-4]</sup>  $\text{PdCO}$  and  $\text{PdCO}^-$  were also investigated by rotational spectroscopy and anion photoelectron spectroscopy in the gas phase.<sup>[5-7]</sup> The geometry and electronic properties of a single CO adsorption on neutral and charged palladium clusters have been the subject of considerable theoretical studies.<sup>[8-21]</sup> Experimentally, the adsorption of a single CO molecule on charged palladium clusters containing 3—25 metal atoms was studied by infrared multiple photon dissociation (IR-MPD) spectroscopy, which found that palladium clusters exhibit a variety of binding sites for CO including a-top, bridge and hollow positions.<sup>[22]</sup> The investigations on the reactions of small neutral and anionic palladium clusters with CO indi-

cated that palladium clusters are able to bind multiple CO molecules, and the maximum number of CO molecules that can bind to each cluster was determined.<sup>[23-25]</sup> In addition, bond dissociation energies of palladium trimer anion carbonyls,  $\text{Pd}_3(\text{CO})_n^-$  ( $n=1-6$ ) were measured in the gas phase by the energy resolved collision-induced dissociation method.<sup>[26]</sup> Although palladium clusters stabilized by multiple CO ligands were calculated at density functional theory level to investigate effects of ligand coverage on properties such as preferred coordination sites, metal-ligand binding energies and structure,<sup>[27]</sup> and some dinuclear and trinuclear palladium carbonyl cluster anions including  $\text{Pd}_2(\text{CO})_n^-$  ( $n=0-4$ ) and  $\text{Pd}_3(\text{CO})_m^-$  ( $m=0-6$ ) were studied by anion photoelectron spectroscopy,<sup>[25]</sup> the electronic and geometric structures of gaseous palladium carbonyl clusters with multiple CO ligands are relatively unknown.

Infrared photodissociation spectroscopy in conjunction with quantum chemical calculations offers one of the most direct and generally applicable experimental approaches to structural investigation of mass-selected clusters in the gas phase.<sup>[28-40]</sup> Recently, this technique is successfully employed in studying transition-metal

\* E-mail: zpliu@fudan.edu.cn, mfzhou@fudan.edu.cn

Received June 19, 2012; accepted August 19, 2012.

Supporting information for this article is available on the WWW under <http://dx.doi.org/10.1002/cjoc.201200595> or from the author.

† Dedicated to the 80th Anniversary of Chinese Chemical Society.

carbonyl ions and multinuclear metal carbonyl clusters in the gas phase.<sup>[41–49]</sup> In the present paper, mass selected homoleptic dinuclear palladium carbonyl cluster cations ranging from  $\text{Pd}_2(\text{CO})_5^+$  to  $\text{Pd}_2(\text{CO})_8^+$  are systematically studied by infrared photodissociation spectroscopy. The cluster structures are assigned and structural and bonding trends are identified by comparison of the experimental spectra with simulated spectra derived from density functional calculations.

## Experimental and Computational Methods

The infrared photodissociation spectra of the homoleptic dinuclear palladium carbonyl cluster cations were measured using a collinear tandem time-of-flight mass spectrometer. The experimental apparatus has been described in detail previously.<sup>[49]</sup> The cluster cations were produced in a Smalley-type laser vaporization supersonic cluster source.<sup>[50]</sup> The 1064 nm fundamental of a Nd:YAG laser (Continuum, Minilite II, 10 Hz repetition rate and 6 ns pulse width) was used to vaporize a rotating palladium metal target. The laser beam with 5–8 mJ/pulse is focused by a lens with a focal length of 300 mm. The palladium carbonyl complexes were produced from the laser vaporization process in expansions of helium gas seeded with 4%–6% CO using a pulsed valve (General Valve, Series 9) at 4–6 MPa backing pressure. After free expansion, the cations were skimmed and analyzed using a Wiley-McLaren time-of-flight mass spectrometer. The clusters of interest were each mass selected and decelerated into the extraction region of a second collinear time-of-flight mass spectrometer, where they were dissociated by a tunable IR laser. The fragment and parent cations were reaccelerated and mass analyzed by the second time-of-flight mass spectrometer.

The cations were detected with a dual microchannel plate detector. The mass signals were amplified with a broadband amplifier and digitized, and were transferred to a computer. Infrared photodissociation spectra were obtained by monitoring the fragment ion yield as a function of the dissociation IR laser wavelength. Typical spectra were recorded by scanning the dissociation laser in steps of  $2 \text{ cm}^{-1}$  and averaging over 250 laser shots at each wavelength. The tunable infrared source used in this study is generated by an KTP/KTA/AgGaSe2 optical parametric oscillator/amplifier system (OPO/OPA, Laser Vision) pumped by a Continuum Powerlite 8000 Nd:YAG laser. The laser pulse energies range from 0.2–1.5 mJ/pulse with an approximate line width of  $1 \text{ cm}^{-1}$ . The infrared laser is loosely focused by a  $\text{CaF}_2$  lens. The wavenumber of the OPO laser is calibrated by a commercial wavemeter (Coherent, WaveMaster).

Quantum chemical calculations were performed to determine the molecular structures and to support the assignment of vibrational frequencies of the observed species. Geometry optimization and harmonic vibra-

tional frequency analysis were performed with the hybrid B3LYP density functional theory (DFT) method in combination with the 6-31+G(d) basis set on C and O atoms and the SDD basis set on Pd.<sup>[51,52]</sup> A scalar relativistic effective core potential was employed for Pd that retains 18 electrons in the valence space. The B3LYP functional is the most popular density functional methods and can provide reliable predictions on the structures and vibrational frequencies of transition metal-containing compounds.<sup>[53]</sup> Previous theoretical studies found that only hybrid density functionals can qualitatively and quantitatively predict the nature of the sigma-donation/pi-back-donation bonding that is associated with the Pd-CO and  $\text{Pd}_2\text{-CO}$  bonds.<sup>[17]</sup> All these calculations were performed using the Gaussian 09 program.<sup>[54]</sup>

In the present study, the computed frequencies are scaled by a factor of 0.98 and are given a  $5 \text{ cm}^{-1}$  full width at half-maximum (fwhm) Lorentzian line shape for comparison to the experimental spectra. We derived this scaling factor by calculating the average value needed to make the experimental and calculated frequencies coincide for the  $\text{Pd}_2(\text{CO})_n^-$  cluster cations studied.

## Results and Discussion

The mass spectrum of palladium carbonyl cluster cations produced by the laser vaporization supersonic cluster source in the  $m/z$  range of 90–500 is shown in Figure 1. The spectrum is composed of two progressions of mass peaks due to mononuclear palladium carbonyl cations  $\text{Pd}(\text{CO})_n^+$  ( $n=1–7$ ) and dinuclear palladium carbonyl cations  $\text{Pd}_2(\text{CO})_n^+$  ( $n=5–8$ ). The small mass peaks interspersed between the  $\text{Pd}(\text{CO})_n^+$  peaks are due to the  $\text{PdC}(\text{CO})_n^+$  complexes. The most notable feature of the spectrum is the significantly enhanced intensity for the  $\text{Pd}(\text{CO})_4^+$ ,  $\text{Pd}(\text{CO})_5^+$  and  $\text{Pd}_2(\text{CO})_6^+$  mass peaks, which occurs independently of the source condition. This suggests that these complexes are relatively more stable than other sizes. Larger multinuclear cluster cations are also observed which are not shown in the spectrum. For each species, the isotopic splitting of palladium can clearly be resolved with their relative intensities matching the natural abundance isotopic distributions. The dinuclear carbonyl cluster cations of interest are each mass-selected and subjected to infrared photodissociation. When the IR laser is on a resonance with the CO stretching of the cluster cations, photofragmentation of the cations involving the loss of CO ligand(s) is observed.

$\text{Pd}_2(\text{CO})_5^+$  The infrared photodissociation spectrum for the  $\text{Pd}_2(\text{CO})_5^+$  cation obtained by monitoring the loss of one CO ligand leading to formation of  $\text{Pd}_2(\text{CO})_4^+$  is shown in Figure 2. The cations fragment only under focused IR laser irradiation, indicating that multiphoton absorption is necessary. The parent ions can be depleted by about 12% at the laser pulse energy

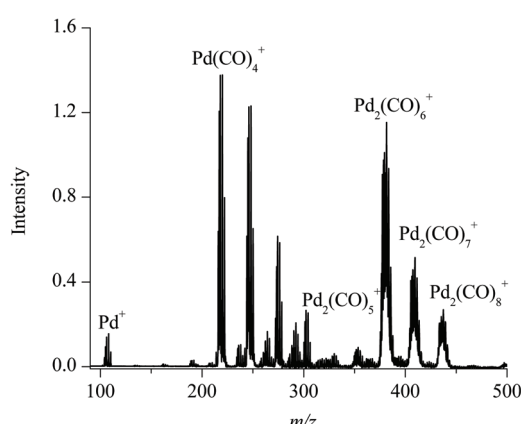


**Figure 1** Mass spectrum of the palladium carbonyl cation complexes produced by pulsed laser vaporization of a palladium metal target in an expansion of helium seeded with carbon monoxide.

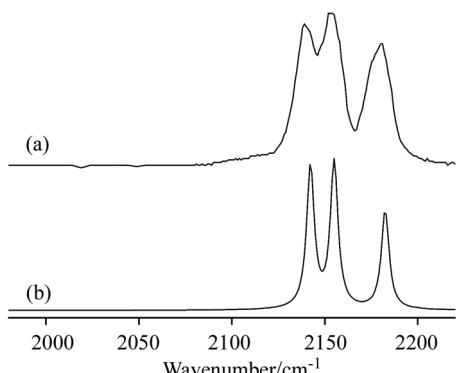


**Figure 2** The experimental and simulated vibrational spectra of the  $\text{Pd}_2(\text{CO})_5^+$  cluster cation in the carbonyl stretching frequency region. The infrared photodissociation spectrum (a) was measured by monitoring the CO fragmentation channel leading to formation of  $\text{Pd}_2(\text{CO})_4^+$ . The simulated spectrum (b) was obtained from scaled harmonic frequencies and intensities for the lowest energy structure calculated at the B3LYP/6-31+G(d)/SDD level.

of about 1 mJ/pulse. The infrared photodissociation spectrum exhibits three broad bands centered at 2139, 2153 and  $2180\text{ cm}^{-1}$ , respectively. No bands in the low frequency region are observed, indicating that the  $\text{Pd}_2(\text{CO})_5^+$  cation involves no bridge bonded carbonyls.

To gain further insight into the structure and spectrum of the  $\text{Pd}_2(\text{CO})_5^+$  cluster cation, quantum chemical calculations using the density functional theory were performed. Geometric optimizations were performed on various possible structures. The most stable structure is shown in Figure 3. The  $\text{Pd}_2(\text{CO})_5^+$  cation was predicted to have  $C_2$  symmetry with three terminal bonded carbonyls and two equivalent very weakly semibridging carbonyls. The computed Pd—C distances to the semibridging CO group are 2.008 and 3.068 Å, respectively. The bond length of the semibridging CO carbonyl ligands (1.136 Å) is only slightly longer than that of the terminal bonded ligands (1.133 and 1.134 Å). The Pd—

Pd bond length is predicted to be 2.770 Å. The calculated infrared spectrum is shown in Figure 2(b), which agrees well with the experimental spectrum. The observed and calculated band positions are compared in Table 1. The  $2180\text{ cm}^{-1}$  band is due to the stretching

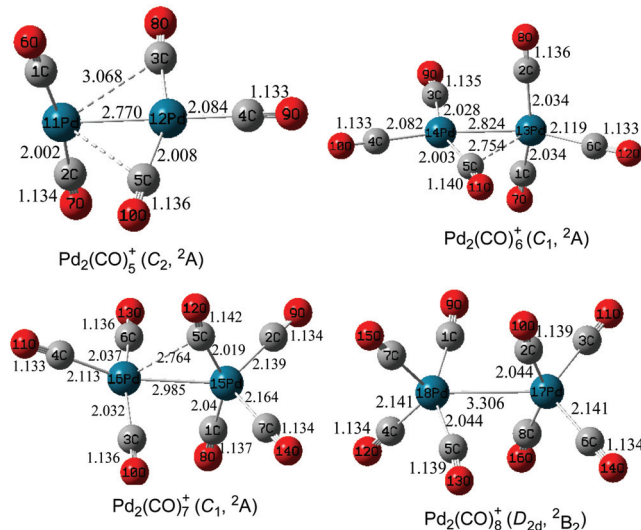


**Figure 3** Geometries and selected bond lengths for the lowest energy structures of the  $\text{Pd}_2(\text{CO})_n^+$  ( $n=5-8$ ) cluster cations calculated at the B3LYP/6-31+G(d)/SDD level.

**Table 1** Comparison of the band positions of the  $\text{Pd}_2(\text{CO})_n^+$  ( $n=5-8$ ) cluster cations measured in the present work to those computed by density functional theory at the B3LYP/6-31+G(d)/SDD level (IR intensities in parentheses in km/mol)

	Exptl.	Calcd. <sup>a</sup>
$n=5$	2139	2142 (850)
	2153	2155 (873)
	—	2157 (0)
	2180	2182 (592)
	—	2199 (1)
	2109	2112 (616)
$n=6$	2140	2140 (810)
	—	2147 (24)
	2164	2162 (342)
	2175	2177 (854)
	—	2190 (21)
	2088	2093 (550)
$n=7$	2141	2135 (218), 2141 (599)
	2159	2154 (221)
	2165	2163 (554)
	2174	2174 (828)
	—	2188 (14)
	2118	2115 (109)
$n=8$	2140	2121 (684×2)
	—	2136 (0)
	2164	2161 (516×2)
	217	2166 (1045)
	—	2185 (0)

<sup>a</sup> The calculated harmonic vibrational frequencies are scaled by a factor of 0.98.

mode of the axial CO ligand of the  $\text{Pd}(\text{CO})_3$  fragment. The  $2139\text{ cm}^{-1}$  band is attributed to the antisymmetric CO stretching vibration of the two semibridging CO ligands. The  $2153\text{ cm}^{-1}$  band is assigned to the antisymmetric stretching mode of the two equivalent CO ligands in the  $\text{Pd}(\text{CO})_2$  fragment.

**Pd<sub>2</sub>(CO)<sub>6</sub><sup>+</sup>** The photodissociation spectrum for the  $\text{Pd}_2(\text{CO})_6^+$  cation obtained by monitoring the loss of one CO ligand is shown in Figure 4. The dissociation efficiency increases by a factor of about two in going from  $\text{Pd}_2(\text{CO})_5^+$  to  $\text{Pd}_2(\text{CO})_6^+$ . Three bands centered at  $2109$ ,  $2140$  and  $2175\text{ cm}^{-1}$  can be clearly resolved in the infrared photodissociation spectrum. In addition, a weak shoulder at the low frequency side of the strong  $2175\text{ cm}^{-1}$  band can also partially be resolved at  $2164\text{ cm}^{-1}$ . As shown in Figure 3, the most stable isomer of  $\text{Pd}_2(\text{CO})_6^+$  is predicted to have a structure involving five terminal CO groups and one weakly semibridging CO group. The optimized structure of the complex has no symmetry, but appears to almost achieve  $C_s$  symmetry. The computed Pd—C distances to the semibridging CO group in  $\text{Pd}_2(\text{CO})_6^+$  are  $2.003$  and  $2.754\text{ \AA}$ , respectively. The Pd—Pd bond distance is calculated to be  $2.824\text{ \AA}$ , slightly longer than that of the  $\text{Pd}_2(\text{CO})_5^+$  cation calculated at the same level of theory. The calculated infrared spectrum of the most stable  $\text{Pd}_2(\text{CO})_6^+$  is compared to the experimental photodissociation spectrum in Figure 4(b). In the simulated spectrum, four bands centered at  $2112$ ,  $2140$ ,  $2162$  and  $2177\text{ cm}^{-1}$  can be resolved to have appreciable IR intensities, which agree well with the experimentally observed spectrum (Table 1). The  $2109\text{ cm}^{-1}$  band is assigned to the stretching vibration of the semibridging carbonyl ligand. The  $2140\text{ cm}^{-1}$  band belongs to the antisymmetric stretching mode of the C(1)—O(7) and C(2)—O(8) ligands (Figure 3). The  $2175\text{ cm}^{-1}$  band is attributed to

the antisymmetric stretching vibration of the C(4)—O(10) and C(6)—O(12) ligands. The  $2164\text{ cm}^{-1}$  band is due to a symmetric stretching mode involving all the carbonyl ligands.

**Pd<sub>2</sub>(CO)<sub>7</sub><sup>+</sup>** The  $\text{Pd}_2(\text{CO})_7^+$  cation complex dissociates quite efficiently. The parent ions can be depleted by more than 30% and are able to lose up to two CO ligands with the focused laser beam. The infrared photodissociation spectrum of  $\text{Pd}_2(\text{CO})_7^+$  obtained by monitoring the loss of one CO ligand is illustrated in Figure 5. The spectrum exhibits five bands with band positions at  $2088$ ,  $2141$ ,  $2159$ ,  $2165$  and  $2174\text{ cm}^{-1}$ . The  $\text{Pd}_2(\text{CO})_7^+$  cluster cation was predicted to have a structure involving six terminal CO groups and one weakly semibridging CO group (Figure 3). The computed Pd—C distances to the semibridging CO group are  $2.019$  and  $2.764\text{ \AA}$ , respectively. The Pd—Pd bond distance is calculated to be  $2.985\text{ \AA}$ , about  $0.161\text{ \AA}$  longer than that of the  $\text{Pd}_2(\text{CO})_6^+$  cation calculated at the same level of theory. The  $\text{Pd}_2(\text{CO})_7^+$  cation without symmetry has seven CO stretching modes that all are IR active. As listed in Table 1, six of them are predicted to have appreciable IR intensities. The calculated spectrum is compared to the experimental spectrum in Figure 5(b). The stretching frequency of semibridged CO ligand is predicted at  $2093\text{ cm}^{-1}$ , slightly higher than the observed value. The predicted  $2135\text{ cm}^{-1}$  band is mainly due to the C(1)—O(8) ligand, while the  $2141\text{ cm}^{-1}$  band originates from the antisymmetric stretching vibration of the C(3)—O(10) and C(6)—O(13) ligands. These two modes cannot be resolved experimentally.

**Pd<sub>2</sub>(CO)<sub>8</sub><sup>+</sup>** The  $\text{Pd}_2(\text{CO})_8^+$  cation is the largest dinuclear cluster complex observed in the mass spectrum, suggesting that it is the coordination saturated cluster. The  $\text{Pd}_2(\text{CO})_8^+$  cation dissociates quite efficiently via loss of one and two CO ligands with moderate laser energy. The infrared photodissociation spectrum

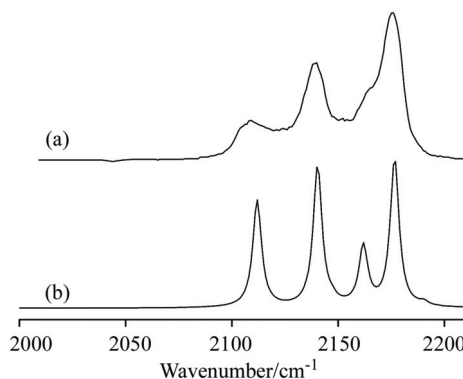


**Figure 4** The experimental and simulated vibrational spectra of the  $\text{Pd}_2(\text{CO})_6^+$  cluster cation in the carbonyl stretching frequency region. The infrared photodissociation spectrum (a) was measured by monitoring the CO fragmentation channel leading to formation of  $\text{Pd}_2(\text{CO})_5^+$ . The simulated spectrum (b) was obtained from scaled harmonic frequencies and intensities for the lowest energy structure calculated at the B3LYP/6-31+G(d)/SDD level.

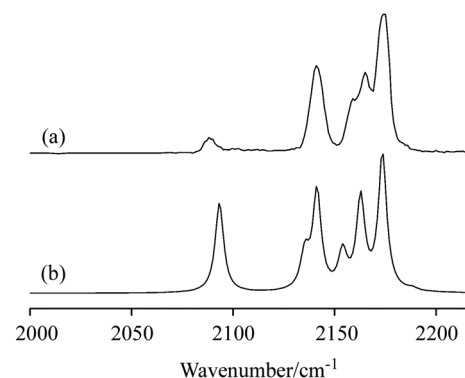


**Figure 5** The experimental and simulated vibrational spectra of the  $\text{Pd}_2(\text{CO})_7^+$  cluster cation in the carbonyl stretching frequency region. The infrared photodissociation spectrum (a) was measured by monitoring the CO fragmentation channel leading to formation of  $\text{Pd}_2(\text{CO})_6^+$ . The simulated spectrum (b) was obtained from scaled harmonic frequencies and intensities for the lowest energy structure calculated at the B3LYP/6-31+G(d)/SDD level.

of  $\text{Pd}_2(\text{CO})_8^+$  obtained by monitoring the loss of one CO ligand is shown in Figure 6. The spectrum recorded via monitoring both fragmentation channels is essentially the same. The spectrum exhibits four bands at 2118, 2140, 2164 and  $2174\text{ cm}^{-1}$ . Density functional calculations predict that the  $\text{Pd}_2(\text{CO})_8^+$  cluster cation has a ground state with  $D_{2d}$  symmetry (Figure 3). The calculated infrared spectrum is compared to the experimental spectrum in Figure 6(b). The experimental spectrum agrees with the calculated spectrum except that the calculated band positions are slightly lower than the observed values. This indicates that the Pd—CO bonding is overestimated while the Pd—Pd bonding is underestimated. The DFT/B3LYP calculations are expected to give relatively poor prediction on  $\text{Pd}_2(\text{CO})_8^+$  with weak Pd-Pd bonding. The  $2140\text{ cm}^{-1}$  band is assigned to the doubly degenerate antisymmetric stretching mode (e) involving either the C(1)—O(9) and C(5)—O(13) ligands or the C(2)—O(10) and C(8)—O(16) ligands, while the  $2118\text{ cm}^{-1}$  band is due to the antisymmetric stretching mode ( $b_2$ ) involving all these four ligands. The  $2164\text{ cm}^{-1}$  band is attributed to the doubly

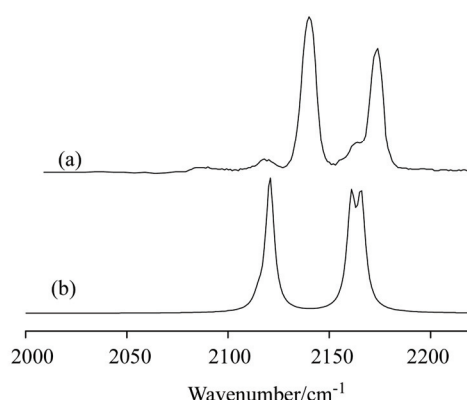


**Figure 6** The experimental and simulated vibrational spectra of the  $\text{Pd}_2(\text{CO})_8^+$  cluster cation in the carbonyl stretching frequency region. The infrared photodissociation spectrum (a) was measured by monitoring the CO fragmentation channel leading to formation of  $\text{Pd}_2(\text{CO})_7^+$ . The simulated spectrum (b) was obtained from scaled harmonic frequencies and intensities for the lowest energy structure calculated at the B3LYP/6-31+G(d)/SDD level.

**Table 2** Bonding characters of the  $\text{Pd}_2(\text{CO})_n^+ (n=5-8)$  cations

Structure	$\Delta E_0(\text{CO})^a$	$\Delta E_0(n\text{CO})^b$	Pd—Pd bond length/ $\text{\AA}$	Group charge <sup>c</sup>		Net spin <sup>d</sup>	
				Pd1	Pd2	Pd1	Pd2
$\text{Pd}_2(\text{CO})_5^+ (C_2, ^2A)$	11.7 (12.9)	27.3	2.770	0.35e	0.65e	0.55e	0.45e
$\text{Pd}_2(\text{CO})_6^+ (C_1, ^2A)$	6.3 (7.0)	23.8	2.824	0.38e	0.62e	0.61e	0.39e
$\text{Pd}_2(\text{CO})_7^+ (C_1, ^2A)$	-0.3 (0.4)	20.3	2.985	0.53e	0.47e	0.38e	0.62e
$\text{Pd}_2(\text{CO})_8^+ (D_{2d}, ^2B_2)$	0.8 (1.7)	17.9	3.306	0.50e	0.50e	0.50e	0.50e

<sup>a</sup> Energy (after zero point energy correction, in kcal/mol) to dissociate one CO from  $\text{Pd}_2(\text{CO})_n^+ (n=5-8)$  cations to form the most stable structure of  $\text{Pd}_2(\text{CO})_{n-1}^+$ . The values without zero point energy correction are listed in parentheses. <sup>b</sup> Averaged energy per CO to remove all CO from  $\text{Pd}_2(\text{CO})_n^+ (n=5-8)$  to form  $\text{Pd}_2^+(^2\Sigma_u) + n\text{CO}$ . <sup>c</sup> Group charge. <sup>d</sup> Net spin populations on the Pd atoms. For the numbering of the atoms, please see Figure 3.

degenerate antisymmetric stretching mode (e) involving either the C(3)—O(11) and C(6)—O(14) ligands or the C(4)—O(12) and C(7)—O(15) ligands, while the  $2174\text{ cm}^{-1}$  band is the antisymmetric stretching mode ( $b_2$ ) involving all these four ligands.

As discussed above, the dinuclear  $\text{Pd}_2(\text{CO})_n^+ (n=5-8)$  cluster cations are produced and experimentally detected. Although the  $\text{Pd}_2(\text{CO})_6^+$  cation is the most intense dinuclear ion product observed in the mass spectrum, the  $\text{Pd}_2(\text{CO})_8^+$  cation is the CO coordination saturated cluster. Thus, the maximum number of bound CO molecules defined as the saturation limit is determined as eight for  $\text{Pd}_2^+$ . The reaction rates of neutral and negative palladium clusters versus CO have been studied using a fast flow reactor.<sup>[23-25]</sup> The saturation limit for  $\text{Pd}_2^-$  was determined to be only five. The neutral palladium dimer is well known to have a  $^3\Sigma_u^+$  ground state with a (core)  $(\pi_u)^4(\sigma_g)^2(\delta_g)^4(\pi_g)^4(\delta_u)^4(\sigma_u)^1(\sigma_g)^1$  electron configuration.<sup>[55,56]</sup> The  $\pi_u$ ,  $\delta_g$ ,  $\pi_g$  and  $\delta_u$  orbitals are combinations of atomic d orbitals which are mainly nonbonding. The doubly occupied  $\sigma_g$  molecular orbital is Pd—Pd  $\sigma$  bonding, which is composed of Pd  $d_z^2$  orbitals (Figure 7). The singly occupied  $\sigma_u$  MO is the corresponding antibonding orbital. Another singly occupied  $\sigma_g$  MO is a bonding orbital composed mainly of Pd 5s atomic orbitals. Accordingly, the neutral palladium dimer has a formal Pd—Pd single bond. Removing one electron from the  $\text{Pd}_2$  HOMO  $\sigma_g$  orbital forms the  $\text{Pd}_2^+$  cation, which has a  $^2\Sigma_u$  ground state with a Pd—Pd half bond. The removal of one  $\sigma_g$  electron reduces the Pd—CO repulsion in the  $\sigma$  space, and enhances the CO to metal  $\sigma$  donation in the cluster cations. In contrast, the addition of an  $\sigma$  electron increases the  $\sigma$  repulsion interaction and reduces the CO to metal  $\sigma$  donation in the cluster anions.

All of the  $\text{Pd}_2(\text{CO})_n^+ (n=5-8)$  cluster cations are

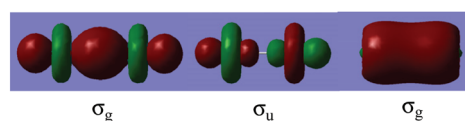


**Figure 7** 3D contours of the doubly occupied and singly occupied  $\sigma$  symmetry molecular orbitals of the  $^3\Sigma_u^+$  ground state  $\text{Pd}_2$  molecule.

characterized to have Pd-Pd bonded structures. The  $n=5\text{--}7$  cluster cations each involves weakly semibridging carbonyl ligand(s), whereas all the carbonyl ligands in the  $n=8$  cluster cation are terminal bonded. The observed CO stretching frequencies of the  $\text{Pd}_2(\text{CO})_n^+$  ( $n=5\text{--}8$ ) cluster cations fall in the range of 2080–2180  $\text{cm}^{-1}$ , very close to the free CO absorption at 2143  $\text{cm}^{-1}$ . This suggests that metal to CO  $\pi$  back bonding is weak in the  $\text{Pd}_2(\text{CO})_n^+$  cation system. Bonding analysis indicates that there is essentially no metal to CO  $\pi$  back donation. The interaction between  $\text{Pd}_2^+$  and CO involves CO to metal  $\sigma$  donation as well as electrostatic bonding that has been observed in “non-classical” transition metal carbonyl cation systems.<sup>[57–59]</sup> As listed in Table 2, the Pd–Pd bond length increases from 2.770 Å in  $\text{Pd}_2(\text{CO})_5^+$  to 3.306 Å in  $\text{Pd}_2(\text{CO})_8^+$ . The natural orbital analysis indicates that these cations each has a doubly occupied  $\sigma$  bonding orbital formed by two Pd 4d orbitals. The singly occupied molecular orbitals are weakly Pd-Pd antibonding in character. Thus, the Pd–Pd bonds in these  $\text{Pd}_2(\text{CO})_n^+$  cluster cations can be regarded as a half bond. On the basis of electron counting rule, the  $n=5\text{--}7$  cluster cations are coordination unsaturated, while the  $n=8$  cluster cation is saturated with both Pd centers having the 18 electron configuration.

The optimized structures of the  $n=5\text{--}7$  complexes are different from the corresponding neutrals. The most stable structures predicted for the  $\text{Pd}_2(\text{CO})_n$  ( $n=2\text{--}7$ ) neutral complexes show at least one CO ligand occupying a bridging position between the two metallic centers.<sup>[27]</sup> These neutral complexes all have a singlet ground state derived from the  ${}^1\Sigma_g^+$  singlet excited state of  $\text{Pd}_2$ , which corresponds to a bond between two Pd 4d<sup>10</sup>5s<sup>0</sup> atoms. The interaction between two 4d<sup>10</sup>5s<sup>0</sup> atoms would presumably form a weak bond.<sup>[60]</sup> Since the  $\sigma_u$  MO is an  $\sigma$  antibonding orbital composed of Pd 5s atomic orbitals, the  ${}^3\Sigma_u^+$  to  ${}^1\Sigma_g^+$  promotion (corresponding to  $[(\sigma_u)^1(\sigma_g)^1]$  to  $[(\sigma_u)^2(\sigma_g)^0]$  excitation) reduces the  $\sigma$  electron density between the two Pd atoms, and hence favors the bridge bonding.

The calculated CO binding energies (dissociate one CO from  $\text{Pd}_2(\text{CO})_n^+$  ( $n=5\text{--}8$ ) cations to form the most stable structure of  $\text{Pd}_2(\text{CO})_{n-1}^+$ ) are listed in Table 2. The binding energies of the  $n=7$  and 8 complexes are much lower than those of  $n=5$  and 6 complexes, suggesting that the  $n=7$  and 8 complexes are very weakly bound complexes.

## Conclusions

Homoleptic dinuclear palladium carbonyl cluster cations of the form  $\text{Pd}_2(\text{CO})_n^+$  with  $n=5\text{--}8$  are produced via a laser vaporization supersonic cluster source in the gas phase. The cations are each mass-selected and their infrared spectra are measured via infrared photodissociation spectroscopy in the carbonyl stretching frequency region. Density functional calculations at the

B3LYP/6-31 + G(d)/SDD level have been performed and the calculated vibrational spectra are compared to the experimental data to identify the gas-phase structures of the clusters. The  $\text{Pd}_2(\text{CO})_5^+$  cation is characterized to have two weakly semibridging CO groups with  $C_2$  symmetry. The  $\text{Pd}_2(\text{CO})_6^+$  and  $\text{Pd}_2(\text{CO})_7^+$  cations are determined to involve one weakly semibridging CO group. The  $\text{Pd}_2(\text{CO})_8^+$  cation is a CO coordination saturated cluster, which is determined to have a  $D_{2d}$  structure with all of the carbonyl groups terminally bonded. Bonding analysis indicates that these cluster cations each have a Pd–Pd half bond. The Pd–Pd distance increases with the number of CO ligands. The results provide important new insight into the structure and bonding mechanisms of palladium carbonyl clusters.

## Acknowledgement

We gratefully acknowledge financial support from National Natural Science Foundation of China (Grant No. 20933030 and 21173053), and National Basic Research Program of China (2010CB732306).

## References

- [1] Darling, J. H.; Ogden, J. S. *J. Chem. Soc., Dalton Trans.* **1973**, 10, 1079.
- [2] Kundig, E. P.; McIntosh, D.; Moskovits, M.; Ozin, G. A. *J. Am. Chem. Soc.* **1973**, 95, 7234.
- [3] Tremblay, B.; Manceron, L. *Chem. Phys.* **1999**, 250, 187.
- [4] Liang, B. Y.; Zhou, M. F.; Andrews, L. *J. Phys. Chem. A* **2000**, 104, 3905.
- [5] Walker, N. R.; Hui, J. K. H.; Gerry, M. C. L. *J. Phys. Chem. A* **2002**, 106, 5803.
- [6] Okabayashi, T.; Yamamoto, T.; Okabayashi, E. Y.; Tanimoto, M. *J. Phys. Chem. A* **2011**, 115, 1869.
- [7] (a) Klopcic, S. A.; Moravec, V. D.; Jarrold, C. C. *J. Chem. Phys.* **1999**, 110, 8986; (b) Chatterjee, B.; Jarrold, C. C.; Raghavachari, K. *J. Chem. Phys.* **2003**, 119, 10591.
- [8] Kobayashi, M. *Bull. Chem. Soc. Jpn.* **1983**, 56, 831.
- [9] Pacchioni, G.; Koutecky, J. *J. Phys. Chem.* **1987**, 91, 2658.
- [10] Blomberg, M. R. A.; Lebrilla, C. B.; Siegbahn, P. E. M. *Chem. Phys. Lett.* **1988**, 150, 522.
- [11] Goursot, A.; Salahub, D. R. *J. Am. Chem. Soc.* **1992**, 114, 7452.
- [12] Rochefort, A.; Fournier, R. *J. Phys. Chem.* **1996**, 100, 13506.
- [13] Dai, D. G.; Roszak, S.; Balasubramanian, K. *J. Chem. Phys.* **1996**, 104, 1471.
- [14] Yudanov, I. V.; Sahnoun, R.; Neyman, K. M.; Rosch, N. *J. Chem. Phys.* **2002**, 117, 9887.
- [15] Yudanov, I. V.; Sahnoun, R.; Neyman, K. M.; Rosch, N.; Hoffmann, J.; Schauermann, S.; Johane, V.; Unterhalt, H.; Rupprechter, G.; Libuda, J.; Freund, H. *J. J. Phys. Chem. B* **2003**, 107, 255.
- [16] Bertin, V.; Agacino, E.; Lopez-Rendon, R.; Poulain, E. *J. Mol. Struct. Theochem.* **2006**, 769, 243.
- [17] Schultz, N. E.; Gherman, B. F.; Cramer, C. J.; Truhlar, D. G. *J. Phys. Chem. B* **2006**, 110, 24030.
- [18] Jiang, L.; Xu, Q. *Chem. Phys.* **2008**, 354, 32.
- [19] Addicoat, M. A.; Buntine, M. A.; Yates, B.; Metha, G. F. *J. Comput. Chem.* **2008**, 29, 1497.
- [20] Zanti, G.; Peeters, D. *Eur. J. Inorg. Chem.* **2009**, 26, 3904.
- [21] (a) Kalita, B.; Deka, R. C. *Eur. Phys. J. D* **2009**, 53, 51; (b) Kalita,

- B.; Deka, R. C. *J. Comput. Chem.* **2010**, *31*, 2476.
- [22] Grue, P.; Fielicke, A.; Meijer, G.; Rayner, D. M. *Phys. Chem. Chem. Phys.* **2008**, *10*, 6144.
- [23] Cox, D. M.; Reichmann, K. C.; Trevor, D. J.; Kaldor, A. *J. Chem. Phys.* **1988**, *88*, 111.
- [24] Hintz, P. A.; Ervin, K. M. *J. Chem. Phys.* **1994**, *100*, 5715.
- [25] Ganterfiir, G.; Schulze Icking-Konert, G.; Handschuh, H.; Eberhardt, W. *Int. J. Mass Spectrom. Ion Processes* **1996**, *159*, 81.
- [26] Spasov, V. A.; Ervin, K. M. *J. Chem. Phys.* **1998**, *109*, 5344.
- [27] Nava, P.; Sierka, M.; Ahlrichs, R. *Phys. Chem. Chem. Phys.* **2004**, *6*, 5338.
- [28] Lisy, J. M. *Int. Rev. Phys. Chem.* **1997**, *16*, 267.
- [29] (a) Ebata, T.; Fujii, A.; Mikami, N. *Int. Rev. Phys. Chem.* **1998**, *17*, 331; (b) Matsuda, Y.; Mikami, N.; Fujii, A. *Phys. Chem. Chem. Phys.* **2009**, *11*, 1279.
- [30] Bieske, E. J.; Dopfer, O. *Chem. Rev.* **2000**, *100*, 3963.
- [31] (a) Duncan, M. A. *Int. J. Mass Spectrom.* **2000**, *200*, 545; (b) Duncan, M. A. *Int. Rev. Phys. Chem.* **2003**, *22*, 407.
- [32] Buck, U.; Huisken, F. *Chem. Rev.* **2000**, *100*, 3863.
- [33] (a) Putter, M.; von Helden, G.; Meijer, G. *Chem. Phys. Lett.* **1996**, *258*, 118; (b) von Helden, G.; van Heijnsbergen, D.; Meijer, G. *J. Phys. Chem. A* **2003**, *107*, 1671; (c) Oomens, J.; Sartakov, B. G.; Meijer, G.; von Helden, G. *Int. J. Mass Spectrom.* **2006**, *254*, 1.
- [34] (a) Robertson, W. H.; Johnson, M. A. *Annu. Rev. Phys. Chem.* **2003**, *54*, 173; (b) Shin, J. W.; Hammer, N. I.; Diken, E. G.; Johnson, M. A.; Walters, R. S.; Jaeger, T. D.; Duncan, M. A.; Christie, R. A.; Jordan, K. D. *Science* **2004**, *304*, 1137; (c) Headrick, J. M.; Diken, E. G.; Walters, R. S.; Hammer, N. I.; Christie, R. A.; Cui, J.; Myshakin, E. M.; Duncan, M. A.; Johnson, M. A.; Jordan, K. D. *Science* **2005**, *308*, 1765; (d) Robertson, W. H.; Diken, E. G.; Price, E. A.; Shin, J. W.; Johnson, M. A. *Science* **2003**, *299*, 1367.
- [35] (a) Bieske, E. J. *Chem. Soc. Rev.* **2003**, *32*, 231; (b) Wild, D. A.; Bieske, E. J. *Int. Rev. Phys. Chem.* **2003**, *22*, 129.
- [36] (a) Asmis, K. R.; Sauer, J. *Mass Spectrom. Rev.* **2007**, *26*, 542; (b) Asmis, K. R.; Brummer, M.; Kaposta, C.; Santambrogio, G.; von Helden, G.; Meijer, G.; Rademann, K.; Woste, L. *Phys. Chem. Chem. Phys.* **2002**, *4*, 1101; (c) Asmis, K. R.; Santambrogio, G.; Brummer, M.; Sauer, J. *Angew. Chem., Int. Ed.* **2005**, *44*, 3122.
- [37] Maitre, P.; MacAleese, L. *Mass Spectrom. Rev.* **2007**, *26*, 583.
- [38] Eyler, J. R. *Mass Spectrom. Rev.* **2009**, *28*, 448.
- [39] Polfer, N. C.; Oomens, J. *Mass Spectrom. Rev.* **2009**, *28*, 468.
- [40] Brodbelt, J. S.; Wilson, J. J. *Mass Spectrom. Rev.* **2009**, *28*, 390.
- [41] Lemaire, J.; Boissel, P.; Heninger, M.; Mauclaire, G.; Bellec, G.; Mestdagh, H.; Simon, A.; Caer, S. L.; Ortega, J. M.; Glotin, F.; Maitre, P. *Phys. Rev. Lett.* **2002**, *89*, 273002.
- [42] (a) Fielicke, A.; von Helden, G.; Meijer, G.; Pedersen, D. B.; Simard, B.; Rayner, D. M. *J. Phys. Chem. B* **2004**, *108*, 14591; (b) Fielicke, A.; von Helden, G.; Meijer, G.; Pedersen, D. B.; Simard, B.; Rayner, D. M. *J. Chem. Phys.* **2006**, *124*, 194305.
- [43] (a) Fielicke, A.; von Helden, G.; Meijer, G.; Simard, B.; Rayner, D. M. *J. Phys. Chem. B* **2005**, *109*, 23935; (b) Fielicke, A.; von Helden, G.; Meijer, G.; Pedersen, D. B.; Simard, B.; Rayner, D. M. *J. Am. Chem. Soc.* **2005**, *127*, 8416; (c) Moore, D. T.; Oomens, J.; Eyler, J. R.; Meijer, G.; von Helden, G.; Ridge, D. P. *J. Am. Chem. Soc.* **2004**, *126*, 14726.
- [44] Ricks, A. M.; Reed, Z. E.; Duncan, M. A. *J. Mol. Spectrosc.* **2011**, *266*, 63.
- [45] (a) Velasquez, J., III; Duncan, M. A. *Chem. Phys. Lett.* **2008**, *461*, 28; (b) Brathwaite, A. D.; Reed, Z. D.; Duncan, M. A. *J. Phys. Chem. A* **2011**, *115*, 10461.
- [46] Velasquez, J., III; Njegic, B.; Gordon, M. S.; Duncan, M. A. *J. Phys. Chem. A* **2008**, *112*, 1907.
- [47] (a) Ricks, A. M.; Bakker, J. M.; Doublerly, G. E.; Duncan, M. A. *J. Phys. Chem. A* **2009**, *113*, 4701; (b) Reed, Z. D.; Duncan, M. A. *J. Am. Soc. Mass Spectrom.* **2010**, *21*, 739; (c) Ricks, A. M.; Reed, Z. D.; Duncan, M. A. *J. Am. Chem. Soc.* **2009**, *131*, 9176; (d) Ricks, A. M.; Gagliardi, L.; Duncan, M. A. *J. Am. Chem. Soc.* **2010**, *132*, 15905.
- [48] (a) Chi, C. X.; Cui, J. M.; Li, Z. H.; Xing, X. P.; Wang, G. J.; Zhou, M. F. *Chem. Sci.* **2012**, *3*, 1698; (b) Wang, G. J.; Cui, J. M.; Chi, C. X.; Zhou, X. J.; Li, Z. H.; Xing, X. P.; Zhou, M. F. *Chem. Sci.* **2012**, DOI: 10.1039/C2SC20947K.
- [49] Wang, G. J.; Chi, C. X.; Cui, J. M.; Xing, X. P.; Zhou, M. F. *J. Phys. Chem. A* **2012**, *116*, 2484.
- [50] Dietz, T. G.; Duncan, M. A.; Powers, D. E.; Smalley, R. E. *J. Chem. Phys.* **1981**, *74*, 6511.
- [51] (a) Becke, A. D. *J. Chem. Phys.* **1993**, *98*, 5648; (b) Lee, C.; Yang, W.; Parr, R. G. *Phys. Rev. B* **1988**, *37*, 785.
- [52] (a) McLean, A. D.; Chandler, G. S. *J. Chem. Phys.* **1980**, *72*, 5639; (b) Krishnan, R.; Binkley, J. S.; Seeger, R.; Pople, J. A. *J. Chem. Phys.* **1980**, *72*, 650.
- [53] (a) Cramer, C. J.; Truhlar, D. G. *Phys. Chem. Chem. Phys.* **2009**, *11*, 10757; (b) Sousa, S. F.; Fernandes, P. A.; Ramos, M. J. *J. Phys. Chem. A* **2007**, *111*, 10439.
- [54] Frisch, M. J.; Trucks, G. W.; Schlegel, H. B.; Scuseria, G. E.; Robb, M. A.; Cheeseman, J. R.; Scalmani, G.; Barone, V.; Mennucci, B.; Petersson, G. A.; Nakatsuji, H.; Caricato, M.; Li, X.; Hratchian, H. P.; Izmaylov, A. F.; Bloino, J.; Zheng, G.; Sonnenberg, J. L.; Hada, M.; Ehara, M.; Toyota, K.; Fukuda, R.; Hasegawa, J.; Ishida, M.; Nakajima, T.; Honda, Y.; Kitao, O.; Nakai, H.; Vreven, T.; Montgomery, J. A. Jr.; Peralta, J. E.; Ogliaro, F.; Bearpark, M.; Heyd, J. J.; Brothers, E.; Kudin, K. N.; Staroverov, V. N.; Kobayashi, R.; Normand, J.; Raghavachari, K.; Rendell, A.; Burant, J. C.; Iyengar, S. S.; Tomasi, J.; Cossi, M.; Rega, N.; Millam, J. M.; Klene, M.; Knox, J. E.; Cross, J. B.; Bakken, V.; Adamo, C.; Jaramillo, J.; Gomperts, R.; Stratmann, R. E.; Yazyev, O.; Austin, A. J.; Cammi, R.; Pomelli, C.; Ochterski, J. W.; Martin, R. L.; Morokuma, K.; Zakrzewski, V. G.; Voth, G. A.; Salvador, P.; Dannenberg, J. J.; Dapprich, S.; Daniels, A. D.; Farkas, O.; Foresman, J. B.; Ortiz, J. V.; Ciosowski, J.; Fox, D. J. *Gaussian 09*, Revision A.02, Gaussian, Inc., Wallingford CT, **2009**.
- [55] Ho, J.; Ervin, K. M.; Polak, M. L.; Gilles, M. K.; Lineberger, W. C. *J. Chem. Phys.* **1991**, *95*, 4845.
- [56] Lombardi, J. R.; Davis, B. *Chem. Rev.* **2002**, *102*, 2431.
- [57] Zhou, M. F.; Andrews, L.; Bauschlicher, C. W. Jr. *Chem. Rev.* **2001**, *101*, 1931.
- [58] (a) Lupinetti, A. J.; Frenking, G.; Strauss, S. H. *Angew. Chem., Int. Ed.* **1998**, *37*, 2113; (b) Lupinetti, A. J.; Strauss, S. H.; Frenking, G. *Prog. Inorg. Chem.* **2001**, *49*, 1.
- [59] Goldman, A. S.; Krogh-Jespersen, K. *J. Am. Chem. Soc.* **1996**, *118*, 12159.
- [60] Morse, M. D. *Chemical Bonding in the Late Transition Metals: The Nickel and Copper Group Dimers*, Vol. 1, JAI Press, Greenwich, CT, **1993**.

(Zhao, X.)